Research Paper

Functional Characterization of Native, High-Affinity GABA_A Receptors in Human Pancreatic β Cells

Sergiy V. Korol [a,1], Zhe Jin [a,1], Yang Jin [a], Amol K. Bhandage [a], Anders Tengholm [b], Nikhil R. Gandasi [a,b], Sebastian Barg [b], Daniel Espes [b], Per-Ola Carlsson [b], Derek Laver [c], Bryndis Birnir [a,*]

[a] Department of Neuroscience, Uppsala University, 75124 Uppsala, Sweden
[b] Department of Medical Cell Biology, Uppsala University, 75124 Uppsala, Sweden
[c] School of Biomedical Sciences and Pharmacy, University of Newcastle, Hunter Medical Research Institute, Callaghan, NSW 2308, Australia

ARTICLE INFO

ABSTRACT

In human pancreatic islets, the neurotransmitter γ-aminobutyric acid (GABA) is an extracellular signaling molecule synthesized by and released from the insulin-secreting β cells. The effective, physiological GABA concentration range within human islets is unknown. Here we use native GABA_A receptors in human islet β cells as biological sensors and reveal that 100–1000 nM GABA elicit the maximal opening frequency of the single-channels. In saturating GABA, the channels desensitized and stopped working. GABA modulated insulin exocytosis and glucose-stimulated insulin secretion. GABA_A receptor currents were enhanced by the benzodiazepine diazepam, the anesthetic propofol and the incretin glucagon-like peptide-1 (GLP-1) but not affected by the hypnotic zolpidem. In type 2 diabetes (T2D) islets, single-channel analysis revealed higher GABA affinity of the receptors. The findings reveal unique GABA_A receptors signaling in human islets β cells that is GABA concentration-dependent, differentially regulated by drugs, modulates insulin secretion and is altered in T2D.

1. Introduction

Pancreatic islet β cells synthesize and release the neurotransmitter GABA. The enzyme glutamic acid decarboxylase (GAD) makes GABA from the amino acid glutamate (Baekkeskov et al. 1990). In β cells, GABA is then stored in synaptic-like microvesicles, in the insulin granules and in the cytoplasm until secreted (Braun et al. 2010; Braun et al. 2004; Kanaani et al. 2015). The roles of GABA in the islets are many; GABA has been linked to regulation of β cells proliferation and β cell mass (Soltani et al. 2011; Tian et al. 2013), the change of α cells into β cells (Ben-Othman et al. 2017; Lawlor et al. 2017; Li et al. 2017), and regulation of hormone secretion (Braun et al. 2010; Li et al. 2015; Taneera et al., 2012). GABA also inhibits immune cells (Bjurstom et al. 2008; Tian et al. 2004) and, thereby, potentially increases β cells survival (Fiorina 2013). Importantly, GAD autoantibodies are associated with the development of type 1 diabetes (T1D) where β cell mass decreases or even disappears whereas in T2D β cell function is compromised (American 2017; Giorda et al. 2016) resulting in abnormally high blood glucose. When the β cell mass declines, the GABA will diminish in the islets making it more difficult for the β cells to influence their own fate. What the physiologically relevant GABA concentrations are in the human islets or what GABA receptor subtypes participate in the signaling is not known (Caicedo 2013; Rodriguez-Diaz and Caicedo 2014; Rorsman and Braun 2013). Importantly, in human islets, insulin-, glucagon- and somatostatin-secreting β, α and δ cells, respectively, all express GABA_A receptors (Braun et al. 2010). This renders the human islet GABA signaling distinct from e.g. signaling in rat and guinea pig islets where functional GABA_A receptors are not expressed in the β cells (Gilon et al. 1991; Jin et al. 2013; Rorsman et al. 1989; Wendt et al. 2004). The GABA_A receptor activity in the brain is enhanced by a number of medicines such as the benzodiazepines, anesthetics and even by the metabolic hormone GLP-1 and its analogue exendin-4 (Korol et al. 2015; Olsen and Sieghart 2008). GLP-1 is a very effective insulin secretagogue (Holst 2007). It is clearly of interest to understand the effects these compounds may have on the GABA_A receptors in the human islet β cells.

Here we use the native GABA_A receptors in β cells as biological sensors for GABA to determine the effective, physiological GABA concentration-range in the human islets. We then characterize β cell-specific high-affinity GABA_A receptors and define their pharmacological profile and further identify their modulation of exocytosis. In T2D, the GABA signaling in the β cells was altered.

* Corresponding author.
  E-mail address: Bryndis.Birnir@neuro.uu.se (B. Birnir).
[1] Contributed equally to the study.

2. Materials and Methods

2.1. Intact Human Pancreatic Islets

Human islets were generously provided by the Nordic Network for Clinical Islet Transplantation, supported by EXODIAB and the Juvenile Diabetes Research Foundation. All procedures were approved by the regional ethics committee in Uppsala and informed consent obtained by appropriate measures from donors or their relatives. Islets were obtained from ND and T2D (HbA1c = 6.5 ± 0.16, mean ± standard error of the mean, SEM) donors and isolated using collagenase digestion and Biocoll gradient centrifugation (Fred et al. 2010), separately for each pancreas. The islets were then hand-picked and cultured free-floating in CMRL 1066 (ICN Biomedicals, Costa Mesa, CA, USA) supplemented with 10 mM HEPES, 2 mM L-glutamine, 50 μg/ml gentamicin, 0.25 μg/ml fungizone (GIBCO, BRL, Gaithersburg, MD, USA), 20 μg/ml ciprofloxacin (Bayer Healthcare, Leverkusen, Germany), and 10 mM nicotinamide at 37 °C in humidified atmosphere containing 5% CO_2, vol/vol and used in the experiments from second day of incubation up to 12 days of culturing.

2.2. Electrophysiological Experiments

The whole-cell patch-clamp configuration was obtained on intact islets using the blind patch-clamp technique (Hamill et al. 1981; Jin et al. 2011; Neher and Sakmann 1976) and single-channel currents were recorded at room temperature (20–22 °C) or at 34 °C. The single intact islet was held by the holding pipette and approached by the recording pipette from the other side (see Fig. 1a). The holding and recording pipettes were made from borosilicate glass. During experiments, the pancreatic islets were perfused with the extracellular solution (mM): 137 NaCl, 5.6 KCl, 2.6 CaCl$_2$, 1.2 MgCl$_2$, 10 HEPES and 20 glucose (pH 7.4 using NaOH) at the rate of 3 ml/min. The intracellular solution consisted of (mM): 135 CsCl, 30 CsOH, 1 MgCl$_2$, 10 EGTA, 5 HEPES and 3 Mg-ATP (pH 7.2 with HCl). Drugs were purchased from Sigma-Aldrich (Steinheim, Germany) or Ascent Scientific (Bristol, UK). Pentobarbital, propofol, GLP-1 and the GABA$_A$R antagonist SR95531 were dissolved in the extracellular solution. Diazepam, zolpidem and the GABA$_A$R antagonist picrotoxin stock solutions were made in dimethyl sulfoxide (DMSO) and then dissolved in the extracellular solution. The final concentration of DMSO was 0.1% and did not affect the recordings (Eghbali et al. 1997). Recordings were done using an Axopatch 200B amplifier, filtered at 2 kHz, digitized on-line at 10 kHz using an analog-to-digital converter and Clampex 10.5 (Molecular Devices, CA, USA) software. The access resistance was monitored and if it changed by >25%, the recording was rejected. The single-channel parameters (amplitude, frequency/opening rate, conductance, open probability P_o, mean current I_{mean} and mean open time T_o) were analyzed by Channel3 (Nicholas Laver, Derek Laver, the University of Newcastle, Australia) and Clampfit 10.5 (Molecular Devices, USA). We used a simplified version of a model, previously established by Jones and Westbrook (Jones and Westbrook 1995) to describe the activation of GABA$_A$ receptors (see Fig. 2a model scheme). Simulations of opening rate and mean open time were generated from this theoretical model using the "Q-matrix" method of Colquhoun and Hawkes (Colquhoun and Hawkes 1981, 1982). We accounted for the effects of missed events due to filtering using the "effective rate constant" method of Blatz and Magleby (Blatz and Magleby 1986) incorporating an event dead-time of 0.1 ms.

2.3. Cytoplasm Harvest and Single-Cell Reverse Transcription Polymerase Chain Reaction (RT-PCR)

The procedure for cytosome harvesting and single-cell RT-PCR have been previously described (Jin et al. 2013). In brief, the cytosome of the cell was harvested in the recording pipette by applying a negative pressure to the pipette at the end of patch-clamp recordings. The harvesting

was terminated immediately before or as soon as the seal broke. The content in the pipette (around 5 μl) was expelled to a 0.2 ml RNase-free PCR tube that was immediately frozen on the dry ice and then stored at −80 °C. The pipette solution and recoding pipettes were autoclaved and the recording electrode was cleaned with 70% ethanol followed by cleaning with RNAase away (Thermo Scientific). The harvested cytosome was subjected to the reverse transcription (RT) step that was performed with Verso™ cDNA synthesis kit (Thermo Scientific). The 20 μl reverse transcription reaction was incubated at 42 °C for 30 min followed by a second incubation at 95 °C for 2 min. PCR was performed in a 10 μl reaction mixture containing 3 μl cDNA, 5× SYBR Green I (Life Technologies), 1× PCR reaction buffer, MgCl2 (3 mM), dNTP (0.3 mM), 1× ROX reference dye, 0.8 U JumpStart Taq DNA polymerase (Sigma-Adrich; Jin et al. 2013) and hormone gene-specific primers. The PCR amplification was performed using the ABI PRISM 7900 HT Sequence Detection System (Applied Biosystems) with an initial denaturation step of 5 min at 95 °C, followed by 45 cycles of 95 °C for 15 s, 60 °C for 30 s and 72 °C for 1 min, and one melting curve step. The primers for hormone genes are insulin (1-forward: AGAGGCCATCAAGCAGATCACTGT, 1-reverse: CTGCGGGCTGCGTCTAG TTG; 2-forward: CCATCAAGCAGATCACTG, 2-reverse: CACTAGG TAGAGAGCTTCC), glucagon (1-forward, AAGGCGAGATTTCCCAGAA GAGG, 1-reverse: ACGTGGCTAGCAGGTGATGTT; 2-forward: GCAA CGTTCCCTTCAAGACAC, 2-reverse: ACTGGTGAATGTGCCCTGTG), and somatostatin (1-forward, GCTTTAGGAGCGAGGTTCGGA, 1-reverse: GGGCATCATTCTCCGTCTGGT; 2-forward: CCCAGACTCCGTCAGTTTCT, 2-reverse: AAGTACTTGGCCAGTTCCTGC). The PCR product was examined by the melting curve and/or run on a 1.5% agarose gel stained with SYBR Gold DNA gel stain (Life Technologies). Total RNA samples from human islets and the intracellular solution or water served as the positive control and negative control, respectively.

2.4. GABA$_A$R Subunits Expression Profile in Human and Mouse β Cells from Single-Cell RNA-seq Data

To examine the GABA receptor subunits expression in human and mouse β cells, two published datasets for islet single-cell RNA-seq from human ND and T2D donors (Segerstolpe et al. 2016; Xin et al. 2016b) and one dataset from mouse (GEO: GSE77980 (Xin et al. 2016a)) were downloaded. The RPKM values (reads per kilobase of transcript per million mapped reads) of GABA receptor subunits from annotated β cells were extracted and plotted.

2.5. Exocytosis Imaging

The islets were dissociated into single cells in 0.0025% trypsin in cell dissociation buffer (Hank's based) for 3–5 min. Cells were washed once in serum-containing medium, plated onto 22-mm polylysine-coated coverslips and allowed to settle overnight. Adenovirus particles adNPY-Venus (Tsuboi et al. 2006) or adNPY-mCherry (Meur et al. 2010) was added and cells were imaged 24–36 h later. Cells selected for experiments expressed the granule marker and appeared healthy. Cells were imaged in a standard solution containing (mM): 138 NaCl, 5.6 KCl, 1.2 MgCl$_2$, 2.6 CaCl$_2$, 20 D-glucose, 5 HEPES (pH 7.4 with NaOH) (Barg et al. 2002; Gandasi and Barg 2014). For depolarization dependent exocytosis experiments, the glucose concentration was 10 mM and the solution supplemented with 2 μM forskolin and 200 μM diazoxide, a K$^+$-ATP-channel opener that prevents glucose-dependent depolarization. Exocytosis was then evoked with high K$^+$ solution (75 mM KCl equimolarly replacing NaCl). High K$^+$ was applied by computer-timed local pressure ejection through a glass pipette similar to those used for patch clamp. All experiments were carried out at ~32 °C. Cells were imaged using a custom-built lens-type total internal reflection fluorescence (TIRF) microscope based on an Axiovert 135 microscope with a 100×/1.45 objective (Carl Zeiss). Excitation was from a DPSS laser at 491 (Cobolt, Stockholm, Sweden), controlled with an

acousto-optical tunable filter (AA-Opto, France) and using dichroic Di01-R488/561 (Semrock) and emission filter FF01-523/610 (Semrock). Scaling was 160 nm per pixel and exposure time 100 ms per frame at 10 frames/s. Exocytosis events were found by eye. The moment of exocytosis was defined as the first significant change (2 standard deviations) from the pre-exocytosis baseline. This definition applied to both types of events, with or without preceding flash. The decay time was then defined as the time from exocytosis until the signal reached less than one third of the amplitude of the event. Traces were read out as DF, defined as average fluorescence in a 0.5 μm circle minus the average fluorescence in a surrounding annulus of 0.8 μm. The point of exocytosis was calculated by fitting the granule fluorescence during exocytosis with a discontinuous function (Eq. (1)), which assumes constant fluorescence before fusion, an inverted exponential decay just after fusion, and finally exponential decay during content release:

$$
\begin{aligned}
&c = A1 \ for \ t < t_1 \\
&C = A2 + (A1 - A2)e^{-\frac{t-t_1}{\tau_1}} \ for \ t_2 > t \geq t_1 \\
&C = A3 + \left(\left(A2 + (A1-A2)e^{-\frac{t_2}{\tau_1}} \right) - A3 \right) e^{-\frac{t-t_2}{\tau_2}} \ for \ t \geq t_2
\end{aligned} \tag{1}
$$

where t is time; c is average fluorescence in a 0.48 μm wide circle at the granule site; A1, A2 and A3 are the fluorescence values at the plateaus; τ1 and τ2 are the decay constants for the fluorescence increase after fusion and content release; and t1 and t2 are the times of fusion and release, respectively.

2.6. GABA Concentration Measurement in Human Islets with GABA ELISA

The individual islets were collected (between 20 and 900 islets from each donor) and after adding 450 μl water into Eppendorf tube containing islets, homogenized by two sessions of 10-second sonication with 1 min break between sonications, keeping the samples on ice during the break. After 2-minute centrifugation of the homogenate at 14000 rpm, 350 μl of the supernatant were collected for subsequent GABA concentration measurement with GABA ELISA (BA E-2500, LDN, Germany), and 50 μl of the same supernatant were taken for protein measurement by improved Lowry assay with the Bio-Rad DCTM Protein Assay (USA). Obtained actual GABA concentration was normalized to protein concentration and expressed in nmol/mg protein for each sample.

2.7. Measurements of Insulin Secretion

Groups of 10–15 size-matched islets were preincubated for 30 min at 37 °C in experimental buffer containing 3 mM glucose followed by 40 min incubation in 500 μl buffer containing 3 or 20 mM glucose with or without GABA and picrotoxin. The incubation medium was subsequently collected, the islets sonicated briefly (1–2 periods of 10 s) in acidic ethanol and frozen overnight. Samples from the medium and the islets were appropriately diluted and analyzed in duplicates for insulin using an immunoassay kit from Mesoscale Discovery (Rockville, MD, USA). Secretion was normalized to insulin content and expressed in relation to that at 20 mM glucose. In some experiments, the islets were placed in a closed 10-μl Teflon tubing perfusion. The chamber was perfused with buffer at a rate of 60 μl/min (AutoMate Scientific, Berkeley, CA). After 30 min of equilibration in buffer with 3 mM glucose, the perfusate was collected in 5-min fractions (Biocollector, Atto Corp, Tokyo, Japan) while changing the glucose concentration, or adding GABA or picrotoxin. Three fractions were collected for each condition and analyzed for insulin. The results are presented as one data point per condition, which represents the average of the last two fractions at that condition. The first fraction was excluded since it was influenced by the preceding condition.

2.8. Statistical Analysis

Statistical analysis was performed using the two-tailed unpaired Student's t-test and Mann-Whitney test (for two groups comparison), one-way ANOVA and Kruskal-Wallis ANOVA on ranks (for multiple comparisons) using GraphPad Prism 7 software (GraphPad Software, USA). The Tukey method was used to detect the outliers. P values < 0.05 were considered statistically significant. All data are presented as mean ± SEM and plotted with GraphPad Prism 7.

3. Results

3.1. GABA-Activated Currents in Intact Human Islets

We used whole-cell patch-clamp (Hamill et al. 1981) to study single GABA$_A$ receptor channels in intact islets from nondiabetic (ND) and clinically diagnosed T2D donors (Table S1). The GABA$_A$ receptor is a transmembrane, pentameric plasma membrane protein complex that contains an integral Cl$^-$ ion channel. The channel is normally closed but it opens when GABA binds to the GABA$_A$ receptor. The current through a single GABA$_A$ receptor is the single-channel current and is manifested in the recording by a deflection (step-opening) from baseline where the channels are closed (Eghbali et al. 1997). Cells were blindly selected for recording (Fig. 1a; Jin et al. 2011, Jin et al. 2013) and the cell-type was determined post-hoc by single-cell RT-PCR analysis of the islet hormone transcripts; glucagon (for α cells), insulin (β cells) and somatostatin (δ cells). GABA-activated currents were recorded from 383 cells in islets from 109 donors (Fig. 1a, b), and 93 cells expressing single hormone transcript could be determined from 38 ND and 6 T2D donors (Fig. 1c, Fig. S1a). The majority of identified cells are β cells (Fig. S1a). Cell capacitance measurement revealed no difference in the median size between different cell-types or between cells from ND and T2D islets (Fig. S1b). While the cell-type could not be defined from the size of the cell, the interstitial GABA-activated current characteristics were cell-type specific (Fig. 1b). The GABA$_A$ receptor single-channel currents had low open probability in the α cells in stark contrast to the β cells were the channel openings were prominent. In δ cells, transient, synaptic-like currents were recorded (Fig. S1c).

3.2. GABA-Activated Receptors in β Cells

We further analyzed the GABA-activated single-channel currents in the β cells. GABA$_A$ receptors (GABA$_A$Rs) can be characterized based on conductance, current kinetics and the receptor's pharmacology. We identified two types of GABA$_A$Rs and termed them islet-GABA$_A$ receptor I and II, iGABA$_A$RI and iGABA$_A$RII respectively, based on the single-channel current distributions (Fig. 1d). The currents were inhibited by picrotoxin, a specific GABA$_A$R antagonist. Representative traces of the currents recorded from ND or T2D islet β cells activated by sequentially applied GABA concentrations are shown in Fig. 1e. When activated by interstitial GABA, the single-channel current varied linearly with the membrane potential and the cord conductance for the iGABA$_A$RI and RII channels were 37 pS and 76 pS (Fig. 1f), respectively.

GABA is released from β and δ cells (Braun et al. 2010) and the interstitial concentration will vary with the physiological activity of the islet. In plasma from ND and T2D donors the GABA concentration was similar, 516 ± 30 nM (n = 10) and 480 ± 28 nM (n = 13), respectively. Currently it is not known what the effective GABA concentration is in the islets. We, therefore, applied a range of GABA concentrations to islets, from 1 to 10^4 nM, to open the channels and examined the effects of GABA on the channel activation, conductance and kinetics (Figs. 1, 2). In ≥10 nM GABA, GABA-activated Cl$^-$ currents were evoked. The average conductance of single iGABA$_A$R channel was generally not dependent on the GABA concentration (Fig. 1g) but, interestingly, the 100 nM GABA-activated iGABA$_A$RI conductance (55 ± 5 pS) recorded in islets from T2D donors was significantly larger than the conductance
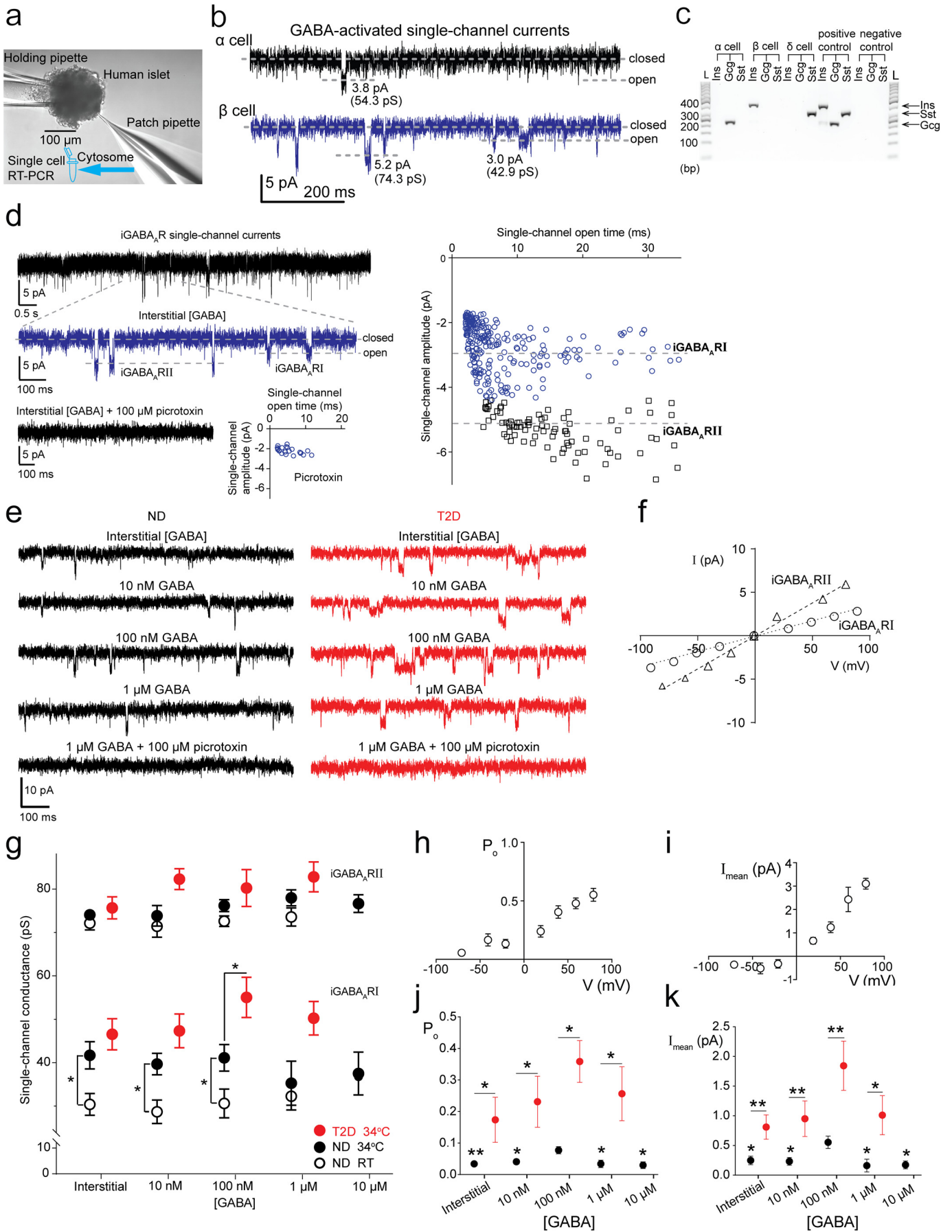
recorded in islets from ND donors (41 ± 3 pS, P < 0.05). All GABA-activated currents were inhibited by the $GABA_AR$ antagonists picrotoxin (100 μM) or SR95531 (100 μM). We also examined effects of temperature on the channels as $GABA_ARs$ commonly have a number of subconductance states (Gage and Chung 1994; Verdoorn et al. 1990). The average conductance of single $iGABA_ARI$ channels was temperature dependent and increased by a factor of 1.3 in interstitial, 10 and 100 nM GABA as the temperature was raised from RT (20–22 °C) to 34 °C (Fig. 1g).

The membrane potential of β cells can vary over a wide range (Braun et al. 2010; Rorsman and Braun 2013). We examined how the open probability (P_o) of the $iGABA_AR$ channels varied with membrane potential displacement away from the chloride reversal potential (E_{Cl}^-). We have previously shown for $GABA_AR$ channels that it is the displacement from the chloride reversal, and not the exact potential value, that determines the conductance characteristics (Birnir et al. 1994). The P_o of the channels is related to both the frequency of openings and the mean open time (T_o) for the channels. The average P_o of the GABA-activated $iGABA_ARs$ was potential dependent and increased with positive membrane potential displacements (Fig. 1h). The mean current (I_{mean}) is related to both the conductance and the P_o of the channels. It is the ensemble of GABA-activated currents in the cell. The I_{mean} was outwardly rectifying (Fig. 1i) revealing that the $iGABA_AR$ effect on the membrane potential increases as the membrane potential is depolarized past the E_{Cl}^-. At these potentials, opening of $iGABA_AR$ channels promotes repolarization of the membrane potential whereas at potentials more negative than E_{Cl}^-, activation of $iGABA_AR$ channels contributes to the excitation of the β cells. We further examined if the I_{mean} and the P_o of the channels were regulated by either GABA concentration or T2D (pipette potential Vp = −70 mV). Interestingly, both 100 nM GABA and T2D significantly (P < 0.05) enhanced P_o (Fig. 1j) and I_{mean} (Fig. 1k) of the $iGABA_AR$ channels.

3.3. In Diabetes iGABA_ARs are Supersensitive to GABA

As the effects on P_o and I_{mean} can only be partially explained by modulation of channel conductance we examined further the kinetic properties of the channels. GABA increased the rate (frequency) of $iGABA_AR$ channel openings in islets from both ND and T2D donors but did not affect the mean open times T_o. Importantly, the frequency of openings was significantly increased in islets from T2D donors resulting in higher apparent affinity for GABA (Fig. 2). At saturating GABA concentrations, the channels desensitized i.e. stopped working (Fig. 2). The data could be fitted with a model (Fig. 2a) comprised of 3 closed states: a GABA-free (C), GABA-bound state primed for channel opening (C*) and a GABA-bound desensitized state (C_d). The model has two open states where of one (O_S) represents spontaneous openings and the other (O_G) occurs in the GABA-primed state. For $iGABA_ARI$, the maximal rate (frequency) of channel openings was in 100 nM GABA, but the opening rate decreased at micromolar concentrations (Fig. 2b, c). The apparent affinity for GABA (K_a) at room temperature (RT) was 20 nM for $iGABA_ARI$, which was significantly lower (P < 0.05) than 65 nM for

$iGABA_ARII$. Both channel types have similar equilibrium constants for desensitization (K_d), in the micromolar range. The T_o of $iGABA_ARI$ was 3-fold lower (P < 0.05) than for $iGABA_ARII$ and this is reflected in the closing rates (k_c). The opening rates of the $iGABA_ARs$ were similar in interstitial and 10 nM GABA suggesting that the interstitial GABA concentration under our experimental conditions is about 10 nM. Raising the temperature to 34 °C resulted in a 2-fold reduction in T_o for $iGABA_ARI$ but no change in opening rate. However, for $iGABA_ARII$, raising the temperature to 34 °C had no effect on T_o but did increase K_a 23-fold and shifted the peak opening rate from 100 nM to 1 μM GABA (Fig. 2a, c). Interestingly, this shift in GABA activation was associated with the appearance of a non-zero baseline in the opening rate in the [GABA] range 10–100 nM, indicating the presence of spontaneous channel openings.

In islets from T2D donors, the data were described by the same model and had similar T_o and K_d as those from ND donors (Fig. 2d, e). However, the K_a for GABA activation of the $iGABA_ARs$ was reduced at RT by 6-fold for $iGABA_ARI$ and at 34 °C by ~3-fold for $iGABA_ARI$ and 300-fold for $iGABA_ARII$. In addition, the opening rate of the $iGABA_ARI$ was significantly higher than recorded in islets from ND donors. Together the results show that in T2D the functional response of the $iGABA_ARI$ and II in pancreatic islets is altered. Furthermore, the total GABA content in ND and T2D islets was significantly different (P < 0.05) being 7.7±2.2 nmol/mg protein (n = 7) and 1.6±0.5 nmol/mg protein (n = 6), respectively.

We investigated further at the single cell transcriptome level if changes in expression of $iGABA_AR$ subunits had occurred. Data from single cell RNA sequencing (GEO: GSE81608 and ArrayExpress: E-MTAB-5060) shown in Fig. 2f revealed that the profile of the expressed $GABA_A$ subunits is altered in β cells from T2D (n = 395 cells) as compared to ND (n = 376 cells) donors. The classical $GABA_B$ receptor is not expressed in the β cells as only one, $GABA_BR1$, of the required two subunits of the dimeric $GABA_B$ receptor (Xu et al. 2014) was expressed in the cells (Fig. S2a).

3.4. GABA Shapes Insulin Exocytosis and Secretion

We examined the effect of GABA on insulin granule exocytosis using the total internal reflection fluorescence (TIRF) microscopy on cells expressing the fluorescent granule-marker neuropeptide-Y (NPY)-Venus. Depolarization of the cells by local application of 75 mM K^+ caused a fraction of the granules to undergo exocytosis, detected as sudden disappearance of fluorescence when NPY-Venus was released (Figs. 3a–c). Exocytosis corresponding to ~210 granules/min for an average-sized cells was observed in control ($3.5 \pm 0.4 \cdot 10^{-3} \cdot \mu m^{-2} \cdot s^{-1}$, n = 6), which decreased to ~150 granules/min in presence of 100 nM GABA ($2.5 \pm 0.6 \cdot 10^{-3} \cdot \mu m^{-2} \cdot s^{-1}$, p < 0.05, n = 7, Figs. 3c–e). The loss of NPY-Venus from individual granules was somewhat faster in presence of GABA compared with control (0.86 ± 0.09 vs 1.28 ± 0.13 s, P < 0.024, Wilcoxon Signed Rank test; n = 119 and 96 granules; Fig. 3c, f, and g). Release was usually preceded by a transient fluorescence increase ($84 \pm 3\%$ in control, n = 119, Fig. 3f), which marks the

---

Fig. 1. Characterization of $GABA_A$ receptor ($iGABA_AR$) single-channel currents in human pancreatic islet β cells. (a) Experimental set-up showing the process of single-channel current recording in intact human islet followed by single-cell RT-PCR. (b) Interstitial GABA-activated single-channel currents in α and β cells. Closed and open states of the single channels are marked with corresponding dash lines. Amplitudes of the currents (in pA) through and corresponding conductances (in pS) of the single channels are indicated. Vp = −70 mV for both cell. (c) Agarose gel showing islet hormone gene expression in single cells from intact islets. Ins, insulin; Gcg, glucagon; Sst, somatostatin; L, ladder; bp, base pair. (d) $iGABA_A$ single-channel currents, and currents at expanded time scale (blue trace) identifying two types of $iGABA_ARs$, $iGABA_ARI$ and II. Scatter plots of $iGABA_AR$ single-channel current amplitudes versus their open times show two populations of $iGABA_ARs$ in a β cell. $GABA_AR$ antagonist picrotoxin inhibited $iGABA_ARs$ (lowest panel). (e) $iGABA_AR$ single-channel currents in a β cell activated first by interstitial GABA and then by sequentially applied GABA concentrations (10–1000 nM) to the islet from ND or T2D donor. The currents were then inhibited by picrotoxin. Vp = −70 mV, 34 °C and scale bars are common for the current recordings. (f) Current-voltage relationships for $iGABA_ARs$ at room temperature (RT). (g) Single-channel conductance of $iGABA_ARI$ and II as a function of GABA concentration ([GABA]) in islets from ND (black symbols) and T2D (red symbols) donors at RT (open symbols) and 34 °C (filled symbols). Data are mean ± SEM from 3 to 11 cells. Unpaired Student's t-test, *P < 0.05. (h and i) Open probability (P_o) of and mean current (I_{mean}) through the $iGABA_ARs$ as a function of the membrane potential at 34 °C. Data are mean ± SEM from 4 to 10 cells. (j and k) P_o of and absolute I_{mean} through $iGABA_ARs$ as a function of [GABA] for ND (black symbols) and T2D donors (red symbols). Data from 3 to 8 cells at 34 °C, Vp = −70 mV. Unpaired Student's t-test for intergroup comparisons and one-way ANOVA multiple comparisons versus control group (100 nM GABA) with Bonferroni post hoc test within ND group; *P < 0.05, **P < 0.01. SEM is shown if the range is larger than the symbol.
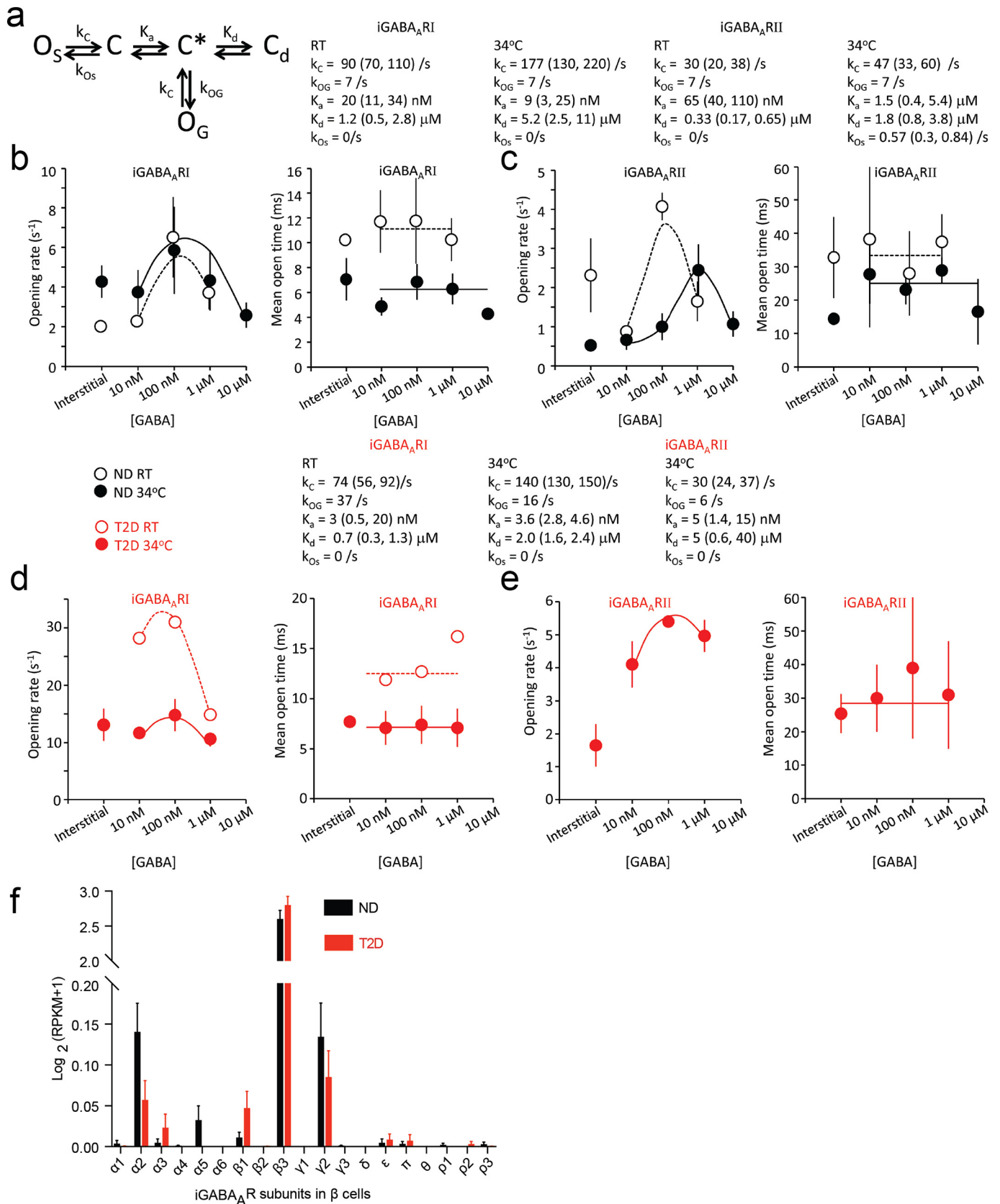
Fig. 2. Kinetic modeling of iGABA$_A$RI and II and expression pattern of iGABA$_A$R subunits in β cells. (a) A kinetic model describing iGABA$_A$R channel behavior in the pancreatic islet β cells. (b and c) Fitting the kinetic model from (a) (curves) to the opening rate and mean open time (T_o) of iGABA$_A$RI and iGABA$_A$RII from ND donors at RT (n = 7 and n = 4, respectively) and at 34 °C (n = 8 and n = 8, respectively). (d and e) Corresponding opening rate and mean open time (T_o) for iGABA$_A$RI and iGABA$_A$RII from T2D donors and fit of the model in (a) to the data at RT (n = 1) and at 34 °C (n = 3). (f) Expression pattern of iGABA$_A$R subunits in single β cells from ND and T2D donors. The expression level was expressed as log$_2$(RPKM+1) and data were presented as mean ± SEM. RPKM, reads per kilobase of transcript per million mapped reads.
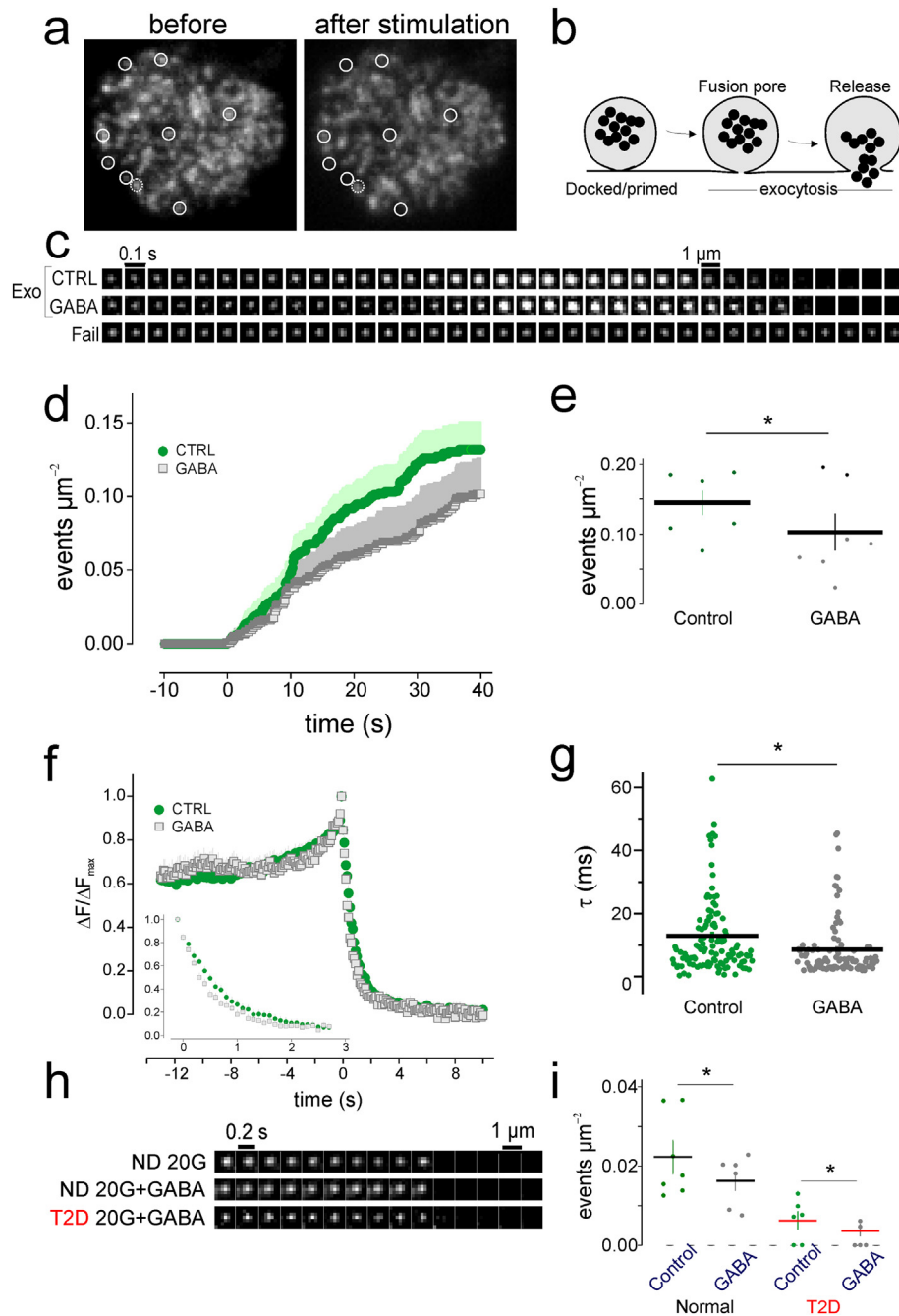
Fig. 3. Effect of GABA on insulin-granule exocytosis in human islets. (a) TIRF image showing labeled granules in a cell before and after application of 75 mM K$^+$. (b) Diagram of docked and primed insulin granules undergoing exocytosis. (c) Single insulin granule exocytotic events from islet cells were triggered by addition of 75 mM K$^+$. The cells expressed NPY-Venus as a granule label in the absence (CTRL) and presence of 100 nM GABA. Fail, non-responding granule which failed to undergo exocytosis. (d) Cumulative number of events per area in the presence and absence of GABA. (e) Analysis of (d) showed significantly decreased number of events per area in the presence of GABA. (f) Average fluorescence intensity and decay of granule fluorescence (inset) from 7 cells per condition in the presence and absence of GABA. (g) The decay constant τ was significantly larger (slower fluorescence decay) in control cells. (h) Single insulin granule exocytotic events from islet cells expressing NPY-mCherry under indicated conditions. 20G, 20 mM glucose. (i) Cumulative number of events per area under indicated conditions. *P < 0.05.

opening of a fusion pore that is too narrow to allow peptide release (Obermuller et al. 2005; Tsuboi and Rutter 2003). No changes were detected in the rising phase of the fluorescence signal, which reflects the fusion pore life-time (Fig. 3f).

We also recorded exocytosis in cells bathed in 20 mM glucose for >10 min, as during 2nd phase insulin secretion. In cells from two ND donors, exocytosis was $0.11 \pm 0.02 \cdot 10^{-3} \cdot \mu m^{-2} \cdot s^{-1}$ (n = 7), corresponding to ~7 granules per minute. With GABA present, exocytosis decreased slightly to $0.095 \pm 0.01 \cdot 10^{-3} \cdot \mu m^{-2} \cdot s^{-1}$ (~5 granules/min, P < 0.05, n

= 6). A similar effect was seen in islet cells from one T2D donor with $0.031 \pm 0.010 \cdot 10^{-3} \cdot \mu m^{-2} \cdot s^{-1}$ (~2 granules/min) in control compared with $0.019 \pm 0.008 \cdot 10^{-3} \cdot \mu m^{-2} \cdot s^{-1}$ (~1 granules/min) with GABA (p < 0.05, Fig. 3h, i). Taken together these data suggest that GABA decreases the rate of exocytosis in β cells. In glucose-stimulated islets, the modulatory effect of GABA on insulin secretion was more complex (Fig. S3) and is in line with the influence of paracrine factors (Caicedo 2013) and differences in electrophysiological behavior of isolated versus islet β-cells (Rorsman and Ashcroft 2018).

### 3.5. iGABA$_A$Rs are Selectively Modulated by Drugs

Many central nervous system (CNS) drugs commonly used clinically are thought to target only neuronal GABA$_A$Rs (Hanson et al. 2008; Olsen and Sieghart 2009; Sieghart 2015). We examined if a benzodiazepine (diazepam), anesthetics (propofol, pentobarbital) and a hypnotic (zolpidem) also modulated the iGABA$_A$Rs (Fig. 4a). Diazepam and zolpidem bind to receptors containing the γ2 GABA$_A$R subunit while zolpidem is, additionally, highly selective for receptors containing the α1 GABA$_A$R subunit. Propofol and pentobarbital potentiate most CNS GABA$_A$R subtypes. In the human islets, importantly, only zolpidem (100 or 200 nM) did not modulate the iGABA$_A$R currents (Fig. 4a). The results are in agreement with the GABA$_A$R subunit expression profile of the β cells (see Fig. 2f).

We further examined if GLP-1, a peptide secreted by L-cells in the gut and enhances insulin secretion, modulated the iGABA$_A$Rs. GLP-1 (50 pM) increased the frequency of the iGABA$_A$RI channel openings (Fig. 4b). Remarkably, the current enhancement by GLP-1 remained, al-beit at a reduced level, when the GLP-1 application was terminated (Fig. 4b). This long-lasting current enhancement was also recorded for iGABA$_A$Rs in an islet from T2D individual.

4. Discussion

The results identify the physiological, submicromolar GABA concentration range in human islets and characterize unique human β cell-specific GABA$_A$Rs, that, when activated, decrease the rate of exocytosis in β cells and modulate glucose-stimulated insulin secretion. We further show that common CNS drugs like diazepam, propofol, pentobarbital but not zolpidem, modulate the receptors and, thereby, highlight the caution that must be taken when considering these types of CNS medicines for people with diabetes. The results also provide a rationale for developments with focus on β cell-specific GABA$_A$R drugs. In accordance with the decreased total GABA content in islets from T2D donors, the induction of the very high-affinity iGABA$_A$R in T2D is likely to be a consequence of the disease and a compensatory response to maintain normal islet functions.
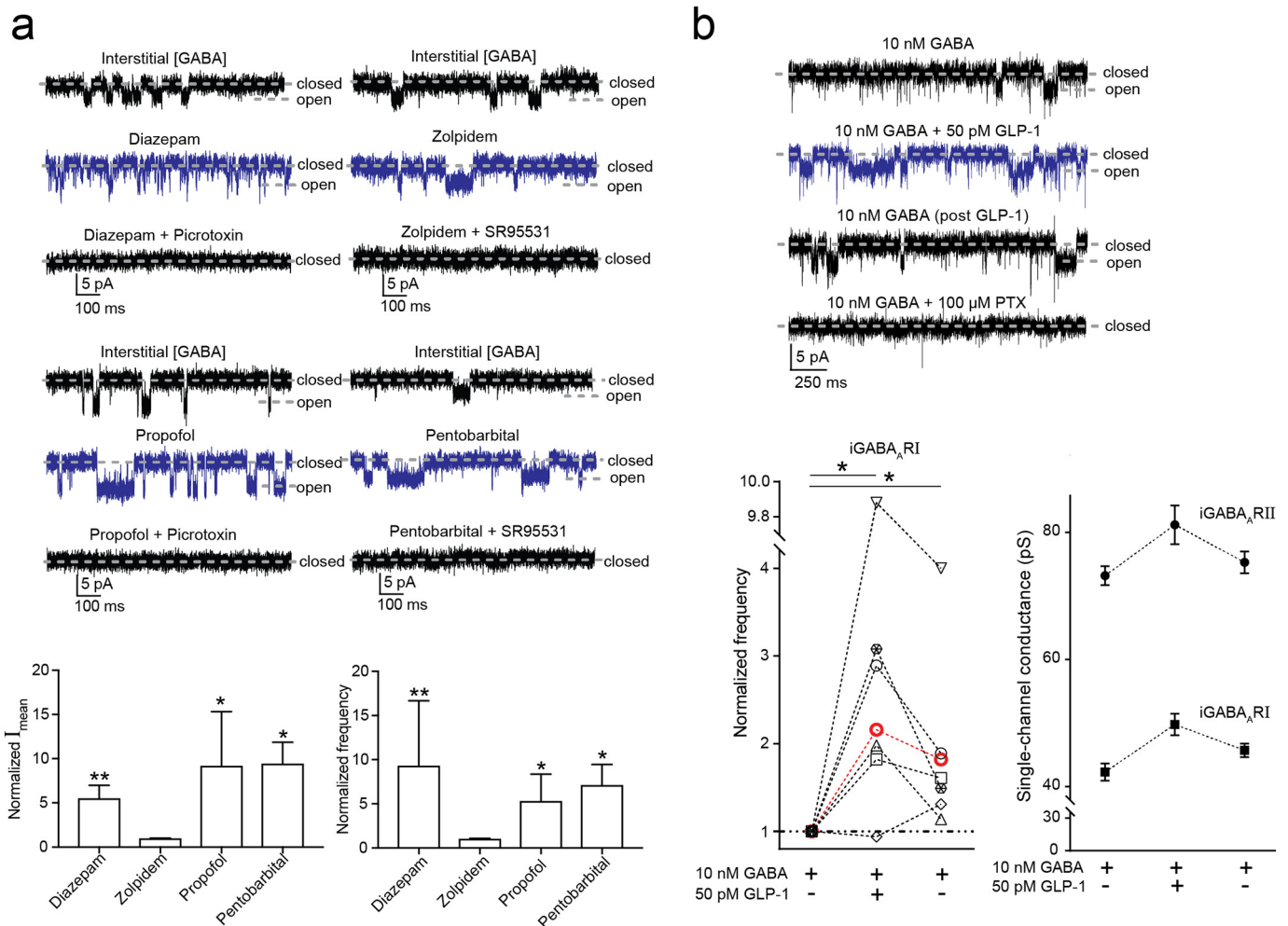
Fig. 4. The modulation of iGABA$_A$R mediated single-channel currents in β cells by GABA$_A$R modulators and GLP-1. (a) Top: iGABA$_A$R-mediated single-channel currents recorded from islet β cells were enhanced by diazepam (1 μM), propofol (10 μM) and pentobarbital (100 μM) but not zolpidem (200 nM). Picrotoxin (100 μM) and SR95531 (100 μM) inhibited the iGABA$_A$R currents. Lower panel: Diazepam (n = 5), propofol (n = 4) and pentobarbital (n = 4) but not zolpidem (n = 4) significantly increased the mean single-channel current (I_{mean}) and opening frequency of iGABA$_A$Rs (*P < 0.05; **P < 0.01, Mann-Whitney test). Data were presented as mean ± SEM. (b) Top: iGABA$_A$R-mediated single-channel currents recorded from a β cell were potentiated by GLP-1 (50 pM) in the presence of GABA (10 nM). The enhanced channel activity was maintained after GLP-1 washout (post GLP-1) and picrotoxin (PTX; 100 μM) inhibited the currents. Lower panel: The opening frequency of iGABA$_A$RI channels was significantly increased by GLP-1 and after GLP-1 washout it remained significantly higher than that before GLP-1 application (*P < 0.05, n = 6). Each cell is identified by a specific symbol and connected by dashed lines (black, ND; red, T2D). One-way ANOVA multiple comparisons versus control group (before GLP-1 application; Dunn's method). The application of GLP-1 and the following washout did not significantly change the single-channel conductance of either iGABA$_A$RI or iGABA$_A$RII (n = 5). Data were presented as mean ± SEM.

The optimal GABA concentrations for active iGABA$_A$Rs ranged from 100 nM to submicromolar GABA. Our model exhibits GABA-primed closed and GABA-desensitized states like those seen in models for neuronal GABA$_A$R-mediated currents (Jones and Westbrook 1995; Lindquist et al. 2005) albeit with 100-fold higher affinity for GABA in the human islets. In T2D, the iGABA$_A$Rs, high conductance and very effective channels, become supersensitive to GABA. In the human β cells only two functional subtypes of GABA$_A$Rs were identified in contrast to the plethora of receptor types expressed in the brain. In islets from ND donors, the pentameric iGABA$_A$R consist of a combination of α2, α5, β3, γ2 subunits. Clearly a number of combinations are possible but the pharmacological profile of the receptors is consistent with α2β3γ2, α5β3γ2 and α2α5β3γ2 (Olsen and Sieghart 2009). The receptors interact with the intracellular milieu that can further shape their characteristics as was apparent by the long-lasting effects of the GLP-1. In islets from individuals with T2D, potential subtypes include the α2β3γ2 but also α3β3γ2 and α2α3β3γ2 iGABA$_A$R receptors. GABA-activated Cl$^-$ currents have not been recorded in β cells in rodent islets, so far (Jin et al. 2013; Rorsman et al. 1989; Soltani et al. 2011; Wendt et al. 2004). However, in mouse β cells, Ca^{2+} transients are modulated by GABA$_A$R agonists (Soltani et al. 2011) and single-cell transcriptome analysis has detected GABA$_A$R subunit genes in mouse islet β cells (GEO: GSE77980, Fig. S2b). The most prominent genes were α4β3δ whereas no or very low level of the γ2 subunit was detected resulting in, potentially, high-affinity GABA$_A$Rs but with different pharmacological profile from the human receptors e.g. being insensitive to benzodiazepines (Olsen and Sieghart 2009). Single-cell sequencing further showed that human β cells express only one of the two obligatory GABA$_B$R subunits in contrasts to e.g. mice where both subunits are expressed (GEO: GSE77980, Fig. S2c), suggesting that in human β cells, GABA signaling is dominated by the GABA$_A$R.

Together, our findings identify β cells-specific high-affinity GABA$_A$R subtypes and the physiologically relevant GABA concentrations in human islets that together modulate insulin secretion. How activating iGABA$_A$Rs alters cellular signaling and why the GABA content in islets from patients with T2D is reduced is currently not known and needs to be resolved in future experiments.

Conflicts of Interest

B. Birnir has filed a patent application based on findings described in this manuscript (1850201-3). All other authors (SVK, ZJ, YJ, AKB, AT, NRG, SB, DE, POC, DL) declare no conflicts of interest.

Author Contributions

Experimental design, S.V.K., Z.J., Y.J. and B.B.; Electrophysiology, S.V.K., Z.J., Y.J. and B.B.; Insulin release, A.T.; Exocytosis, N.G. and S.B.; Single-cell RT-PCR, Y.J., Z.J., S.V.K. and A.K.B.; RNAseq analysis, Z.J.; Blood collection, D.E. and P.O.C.; Plasma GABA measurement, A.K.B.; Single-channel analysis, S.V.K., Z.J., Y.J., B.B. and D.L.; Single-channel modeling, D.L.; Writing – Original draft, B.B.; Writing – Review & editing, all co-authors.

Acknowledgements

Appendix A. Supplementary Data

Supplementary data to this article can be found online at https://doi.org/10.1016/j.ebiom.2018.03.014.

References

American, A.D., 2017. 2. Classification and diagnosis of diabetes. Diabetes Care 40, S11–S24.

Baekkeskov, S., Aanstoot, H.J., Christgau, S., Reetz, A., Solimena, M., Cascalho, M., Folli, F., Richter-Olesen, H., De Camilli, P., 1990. Identification of the 64K autoantigen in insulin-dependent diabetes as the GABA-synthesizing enzyme glutamic acid decarboxylase. Nature 347, 151–156.

Barg, S., Olofsson, C.S., Schriever-Abeln, J., Wendt, A., Gebre-Medhin, S., Renstrom, E., Rorsman, P., 2002. Delay between fusion pore opening and peptide release from large dense-core vesicles in neuroendocrine cells. Neuron 33, 287–299.

Ben-Othman, N., Vieira, A., Courtney, M., Record, F., Gjernes, E., Avolio, F., Hadzic, B., Druelle, N., Napolitano, T., Navarro-Sanz, S., et al., 2017. Long-term GABA administration induces alpha cell-mediated beta-like cell neogenesis. Cell 168, 73–85 (e11).

Birnir, B., Everitt, A.B., Gage, P.W., 1994. Characteristics of GABA$_A$ channels in rat dentate gyrus. J. Membr. Biol. 142, 93–102.

Bjurstom, H., Wang, J., Ericsson, I., Bengtsson, M., Liu, Y., Kumar-Mendu, S., Issazadeh-Navikas, S., Birnir, B., 2008. GABA, a natural immunomodulator of T lymphocytes. J. Neuroimmunol. 205, 44–50.

Blatz, A.L., Magleby, K.L., 1986. Correcting single-channel data for missed events. Biophys. J. 49, 967–980.

Braun, M., Wendt, A., Birnir, B., Broman, J., Eliasson, L., Galvanovskis, J., Gromada, J., Mulder, H., Rorsman, P., 2004. Regulated exocytosis of GABA-containing synaptic-like microvesicles in pancreatic beta-cells. J. Gen. Physiol. 123, 191–204.

Braun, M., Ramracheya, R., Bengtsson, M., Clark, A., Walker, J.N., Johnson, P.R., Rorsman, P., 2010. Gamma-aminobutyric acid (GABA) is an autocrine excitatory transmitter in human pancreatic beta-cells. Diabetes 59, 1694–1701.

Caicedo, A., 2013. Paracrine and autocrine interactions in the human islet: more than meets the eye. Semin. Cell Dev. Biol. 24, 11–21.

Colquhoun, D., Hawkes, A.G., 1981. On the stochastic properties of single ion channels. Proc. R. Soc. Lond. B Biol. Sci. 211, 205–235.

Colquhoun, D., Hawkes, A.G., 1982. On the stochastic properties of bursts of single ion channel openings and of clusters of bursts. Philos. Trans. R. Soc. Lond. Ser. B Biol. Sci. 300, 1–59.

Eghbali, M., Curmi, J.P., Birnir, B., Gage, P.W., 1997. Hippocampal GABA$_A$ channel conductance increased by diazepam. Nature 388, 71–75.

Fiorina, P., 2013. GABAergic system in beta-cells: from autoimmunity target to regeneration tool. Diabetes 62, 3674–3676.

Fred, R.G., Bang-Berthelsen, C.H., Mandrup-Poulsen, T., Grunnet, L.G., Welsh, N., 2010. High glucose suppresses human islet insulin biosynthesis by inducing miR-133a leading to decreased polypyrimidine tract binding protein-expression. PLoS One 5, e10843.

Gage, P.W., Chung, S.H., 1994. Influence of membrane potential on conductance sublevels of chloride channels activated by GABA. Proc. Biol. Sci. 255, 167–172.

Gandasi, N.R., Barg, S., 2014. Contact-induced clustering of syntaxin and munc18 docks secretory granules at the exocytosis site. Nat. Commun. 5, 3914.

Gilon, P., Bertrand, G., Loubatieres-Mariani, M.M., Remacle, C., Henquin, J.C., 1991. The influence of gamma-aminobutyric acid on hormone release by the mouse and rat endocrine pancreas. Endocrinology 129, 2521–2529.

Giorda, C.B., Russo, G.T., Cercone, S., De Cosmo, S., Nicolucci, A., Cucinotta, D., 2016. Incidence and correlated factors of beta cell failure in a 4-year follow-up of patients with type 2 diabetes: a longitudinal analysis of the BETADECLINE study. Acta Diabetol. 53, 761–767.

Hamill, O.P., Marty, A., Neher, E., Sakmann, B., Sigworth, F.J., 1981. Improved patch-clamp techniques for high-resolution current recording from cells and cell-free membrane patches. Pflugers Arch. 391, 85–100.

Hanson, S.M., Morlock, E.V., Satyshur, K.A., Czajkowski, C., 2008. Structural requirements for eszopiclone and zolpidem binding to the gamma-aminobutyric acid type-A (GABA$_A$) receptor are different. J. Med. Chem. 51, 7243–7252.

Holst, J.J., 2007. The physiology of glucagon-like peptide 1. Physiol. Rev. 87, 1409–1439.

Jin, Z., Jin, Y., Birnir, B., 2011. GABA-activated single-channel and tonic currents in rat brain slices. J. Vis. Exp. (53), e2858 https://doi.org/10.3791/2858.

Jin, Y., Korol, S.V., Jin, Z., Barg, S., Birnir, B., 2013. In intact islets interstitial GABA activates GABA$_A$ receptors that generate tonic currents in alpha-cells. PLoS One 8, e67228.

Jones, M.V., Westbrook, G.L., 1995. Desensitized states prolong GABA$_A$ channel responses to brief agonist pulses. Neuron 15, 181–191.

Kanaani, J., Cianciaruso, C., Phelps, E.A., Pasquier, M., Brioudes, E., Billestrup, N., Baekkeskov, S., 2015. Compartmentalization of GABA synthesis by GAD67 differs between pancreatic beta cells and neurons. PLoS One 10, e0117130.

Korol, S.V., Jin, Z., Babateen, O., Birnir, B., 2015. GLP-1 and exendin-4 transiently enhance GABA$_A$ receptor-mediated synaptic and tonic currents in rat hippocampal CA3 pyramidal neurons. Diabetes 64, 79–89.

Lawlor, N., George, J., Bolisetty, M., Kursawe, R., Sun, L., Sivakamasundari, V., Kycia, I., Robson, P., Stitzel, M.L., 2017. Single-cell transcriptomes identify human islet cell signatures and reveal cell-type-specific expression changes in type 2 diabetes. Genome Res. 27, 208–222.

Li, J., Zhang, Q., Liu, X., Wang, Y., Mao, F., Mao, J., Lu, X., Jiang, D., Wan, Y., Lv, J.Y., et al., 2015. Study of GABA in healthy volunteers: pharmacokinetics and pharmacodynamics. Front. Pharmacol. 6, 260.

Li, J., Casteels, T., Frogne, T., Ingvorsen, C., Honore, C., Courtney, M., Huber, K.V., Schmitner, N., Kimmel, R.A., Romanov, R.A., et al., 2017. Artemisinins target GABA$_A$ receptor signaling and impair alpha cell identity. Cell 168, 86–100 (e115).

Lindquist, C.E., Laver, D.R., Birnir, B., 2005. The mechanism of SR95531 inhibition at GABA receptors examined in human α1β1 and α1β1γ2S receptors. J. Neurochem. 94, 491–501.

Meur, G., Simon, A., Harun, N., Virally, M., Dechaume, A., Bonnefond, A., Fetita, S., Tarasov, A.I., Guillausseau, P.J., Boesgaard, T.W., et al., 2010. Insulin gene mutations resulting in early-onset diabetes: marked differences in clinical presentation, metabolic status, and pathogenic effect through endoplasmic reticulum retention. Diabetes 59, 653–661.

Neher, E., Sakmann, B., 1976. Single-channel currents recorded from membrane of denervated frog muscle fibres. Nature 260, 799–802.

Obermuller, S., Lindqvist, A., Karanauskaite, J., Galvanovskis, J., Rorsman, P., Barg, S., 2005. Selective nucleotide-release from dense-core granules in insulin-secreting cells. J. Cell Sci. 118, 4271–4282.

Olsen, R.W., Sieghart, W., 2008. International union of pharmacology. LXX. Subtypes of gamma-aminobutyric acid$_A$ receptors: classification on the basis of subunit composition, pharmacology, and function. Update. Pharmacol. Rev. 60, 243–260.

Olsen, R.W., Sieghart, W., 2009. GABA$_A$ receptors: subtypes provide diversity of function and pharmacology. Neuropharmacology 56, 141–148.

Rodriguez-Diaz, R., Caicedo, A., 2014. Neural control of the endocrine pancreas. Best Pract. Res. Clin. Endocrinol. Metab. 28, 745–756.

Rorsman, P., Ashcroft, F.M., 2018. Pancreatic beta-cell electrical activity and insulin secretion: of mice and men. Physiol. Rev. 98, 117–214.

Rorsman, P., Braun, M., 2013. Regulation of insulin secretion in human pancreatic islets. Annu. Rev. Physiol. 75, 155–179.

Rorsman, P., Berggren, P.O., Bokvist, K., Ericson, H., Mohler, H., Ostenson, C.G., Smith, P.A., 1989. Glucose-inhibition of glucagon secretion involves activation of GABA$_A$-receptor chloride channels. Nature 341, 233–236.

Segerstolpe, A., Palasantza, A., Eliasson, P., Andersson, E.M., Andreasson, A.C., Sun, X., Picelli, S., Sabirsh, A., Clausen, M., Bjursell, M.K., et al., 2016. Single-cell transcriptome profiling of human pancreatic islets in health and type 2 diabetes. Cell Metab. 24, 593–607.

Sieghart, W., 2015. Allosteric modulation of GABA$_A$ receptors via multiple drug-binding sites. Adv. Pharmacol. 72, 53–96.

Soltani, N., Qiu, H., Aleksic, M., Glinka, Y., Zhao, F., Liu, R., Li, Y., Zhang, N., Chakrabarti, R., Ng, T., et al., 2011. GABA exerts protective and regenerative effects on islet beta cells and reverses diabetes. Proc. Natl. Acad. Sci. U. S. A. 108 (28):11692–11697. https://doi.org/10.1073/pnas.1102715108.

Taneera, J., Jin, Z., Jin, Y., Muhammed, S.J., Zhang, E., Lang, S., Salehi, A., Korsgren, O., Renstrom, E., Groop, L., et al., 2012. Gamma-aminobutyric acid (GABA) signalling in human pancreatic islets is altered in type 2 diabetes. Diabetologia 55, 1985–1994.

Tian, J., Lu, Y., Zhang, H., Chau, C.H., Dang, H.N., Kaufman, D.L., 2004. Gamma-aminobutyric acid inhibits T cell autoimmunity and the development of inflammatory responses in a mouse type 1 diabetes model. J. Immunol. 173, 5298–5304.

Tian, J., Dang, H., Chen, Z., Guan, A., Jin, Y., Atkinson, M.A., Kaufman, D.L., 2013. Gamma-aminobutyric acid regulates both the survival and replication of human beta-cells. Diabetes 62, 3760–3765.

Tsuboi, T., Rutter, G.A., 2003. Multiple forms of "kiss-and-run" exocytosis revealed by evanescent wave microscopy. Curr. Biol. 13, 563–567.

Tsuboi, T., Ravier, M.A., Parton, L.E., Rutter, G.A., 2006. Sustained exposure to high glucose concentrations modifies glucose signaling and the mechanics of secretory vesicle fusion in primary rat pancreatic beta-cells. Diabetes 55, 1057–1065.

Verdoorn, T.A., Draguhn, A., Ymer, S., Seeburg, P.H., Sakmann, B., 1990. Functional properties of recombinant rat GABA$_A$ receptors depend upon subunit composition. Neuron 4, 919–928.

Wendt, A., Birnir, B., Buschard, K., Gromada, J., Salehi, A., Sewing, S., Rorsman, P., Braun, M., 2004. Glucose inhibition of glucagon secretion from rat alpha-cells is mediated by GABA released from neighboring beta-cells. Diabetes 53, 1038–1045.

Xin, Y., Kim, J., Ni, M., Wei, Y., Okamoto, H., Lee, J., Adler, C., Cavino, K., Murphy, A.J., Yancopoulos, G.D., et al., 2016a. Use of the Fluidigm C1 platform for RNA sequencing of single mouse pancreatic islet cells. Proc. Natl. Acad. Sci. U. S. A. 113, 3293–3298.

Xin, Y., Kim, J., Okamoto, H., Ni, M., Wei, Y., Adler, C., Murphy, A.J., Yancopoulos, G.D., Lin, C., Gromada, J., 2016b. RNA sequencing of single human islet cells reveals type 2 diabetes genes. Cell Metab. 24, 608–615.

Xu, C., Zhang, W., Rondard, P., Pin, J.P., Liu, J., 2014. Complex GABA$_B$ receptor complexes: how to generate multiple functionally distinct units from a single receptor. Front. Pharmacol. 5, 12.